Title
Dominant de novo DSP mutations cause erythrokeratodermia-cardiomyopathy syndrome

Journal
Human Molecular Genetics, 25(2)

ISSN
0964-6906

Authors
Boyden, Lynn M
Kam, Chen Y
Hernández-Martín, Angela
et al.

Publication Date
2016-01-15

DOI
10.1093/hmg/ddv481

Peer reviewed

OXFORD

Human Molecular Genetics, 2016, Vol. 25, No. 2 348–357

doi: 10.1093/hmg/ddv481
Advance Access Publication Date: 24 November 2015
Original Article

ORIGINAL ARTICLE

Dominant *de novo DSP* mutations cause erythrokeratodermia-cardiomyopathy syndrome

Lynn M. Boyden[1], Chen Y. Kam[4], Angela Hernández-Martín[5], Jing Zhou[2], Brittany G. Craiglow[2], Robert Sidbury[6], Erin F. Mathes[7], Sheilagh M. Maguiness[8], Debra A. Crumrine[7], Mary L. Williams[7], Ronghua Hu[2], Richard P. Lifton[1], Peter M. Elias[7], Kathleen J. Green[4] and Keith A. Choate[1,2,3,*]

[1]Department of Genetics, [2]Department of Dermatology and [3]Department of Pathology, Yale University School of Medicine, New Haven, CT, USA, [4]Departments of Pathology and Dermatology, Northwestern University Feinberg School of Medicine, Chicago, IL, USA, [5]Department of Dermatology, Hospital Infantil del Niño Jesús, Madrid, Spain, [6]Department of Pediatrics, University of Washington, Seattle, WA, USA, [7]Department of Dermatology, UCSF School of Medicine, San Francisco, CA, USA and [8]Department of Dermatology, University of Minnesota, Minneapolis, MN, USA

*To whom correspondence should be addressed at: 333 Cedar Street. PO Box 208059, New Haven, CT 06520-8059, USA. Tel: +1 2037853912; Email: keith.choate@yale.edu

Abstract

Disorders of keratinization (DOK) show marked genotypic and phenotypic heterogeneity. In most cases, disease is primarily cutaneous, and further clinical evaluation is therefore rarely pursued. We have identified subjects with a novel DOK featuring erythrokeratodermia and initially-asymptomatic, progressive, potentially fatal cardiomyopathy, a finding not previously associated with erythrokeratodermia. We show that *de novo* missense mutations clustered tightly within a single spectrin repeat of *DSP* cause this novel cardio-cutaneous disorder, which we term erythrokeratodermia-cardiomyopathy (EKC) syndrome. We demonstrate that *DSP* mutations in our EKC syndrome subjects affect localization of desmosomal proteins and connexin 43 in the skin, and result in desmosome aggregation, widening of intercellular spaces, and lipid secretory defects. *DSP* encodes desmoplakin, a primary component of desmosomes, intercellular adhesion junctions most abundant in the epidermis and heart. Though mutations in *DSP* are known to cause other disorders, our cohort features the unique clinical finding of severe whole-body erythrokeratodermia, with distinct effects on localization of desmosomal proteins and connexin 43. These findings add a severe, previously undescribed syndrome featuring erythrokeratodermia and cardiomyopathy to the spectrum of disease caused by mutation in *DSP*, and identify a specific region of the protein critical to the pathobiology of EKC syndrome and to DSP function in the heart and skin.

Introduction

Disorders of keratinization (DOK) are a severe and diverse group of skin diseases characterized by generalized or localized scaling frequently associated with significant morbidity and, more rarely, with mortality, particularly in disorders with severe perinatal presentations or associated systemic abnormalities. Over 70 genes have been shown to cause keratinization disorders, yet they explain only a portion of the heritability for DOK, which demonstrate substantial locus and phenotypic heterogeneity. We have established a large cohort of comprehensively phenotyped DOK kindreds, and have employed targeted and exome sequencing to achieve genetic diagnoses and to identify a cohort of subjects without mutation in known genes. Further clinical characterization of these individuals has revealed unique phenotypes, and

Received: September 23, 2015. **Revised and Accepted:** November 16, 2015

these data provide strong evidence for heretofore unrecognized genetic determinants of DOK, and the potential to further advance the molecular understanding of these debilitating disorders.

Desmosomes are intercellular junctions that play a critical role in cell-cell adhesion, tissue integrity, and differentiation in the epidermis. Desmosomal cadherins have extracellular interactions with their counterparts on neighboring cells and intracellular interactions with the armadillo proteins plakophilin and junctional plakoglobin (PKP1-3 and JUP, respectively). PKPs and JUP interact with desmoplakin (DSP), which also binds intermediate filaments (e.g. desmin in muscle cells, keratins in skin, hair, and nails), completing the link between the cytoskeleton and extracellular adhesion plaques (1,2). Desmosomes also interact with microtubules via association of DSP with microtubule-binding protein end-binding 1, modifying microtubule organization and dynamics at sites of cell-cell contact, and mediating localization and function of gap junction proteins, including connexin 43 (Cx43) (3,4). Cx43 is the most widely expressed connexin (5), with expression in cardiomyocytes and smooth muscle cells of the heart (6), and throughout the epidermis, with predominant expression in basal proliferating cells (7).

Results

Clinical phenotypes

Analysis of exome data from the DOK cohort revealed that three subjects (index cases 614, 244 and 380) were heterozygous for tightly clustered missense mutations in the same candidate gene. Upon further examination of these subjects, consistent clinical features were identified that have not previously been observed in other disorders featuring erythrokeratodermia.

Index case 614 was noted to have sparse, coarse hair at birth with otherwise normal skin, but developed an intertriginous eruption shortly after birth, which generalized to become persistent pruritic erythrokeratodermia unresponsive to topical or systemic immunomodulatory agents (methotrexate, prednisone), oral retinoids, and antihistamines (Fig. 1A and B). He experienced failure to thrive, at 3rd percentile for height and 15th percentile for weight at 2.5 years of age. Serum IgE and eosinophil count were normal, as were biochemical and metabolic profiles, save mild zinc deficiency. His palms and soles were slightly thickened with frequent peeling and cracking (Supplementary Material, Fig. S1A), and scalp hair was absent. Histologic examination of the skin showed psoriasiform acanthosis, hypogranulosis and compact orthohyperkeratosis (Fig. 1J). Hearing and vision were normal. Dental exams noted marked enamel defects, with recurrent caries of primary teeth and soft, chalk-like, poorly mineralized enamel. He had onychodystrophy of all nails (Fig. 1G). At age 2 he was noted to have a systolic murmur and echocardiographic evaluation revealed mild left ventricular dilation. At age 3 he had an acute episode of dyspnea, leading to the discovery of cardiomegaly and pulmonary edema on a chest radiograph. Subsequent echocardiography showed marked left atrial and ventricular dilation and right ventricular dilation with an ejection fraction of 20%, and he died of heart failure after a brief hospitalization.

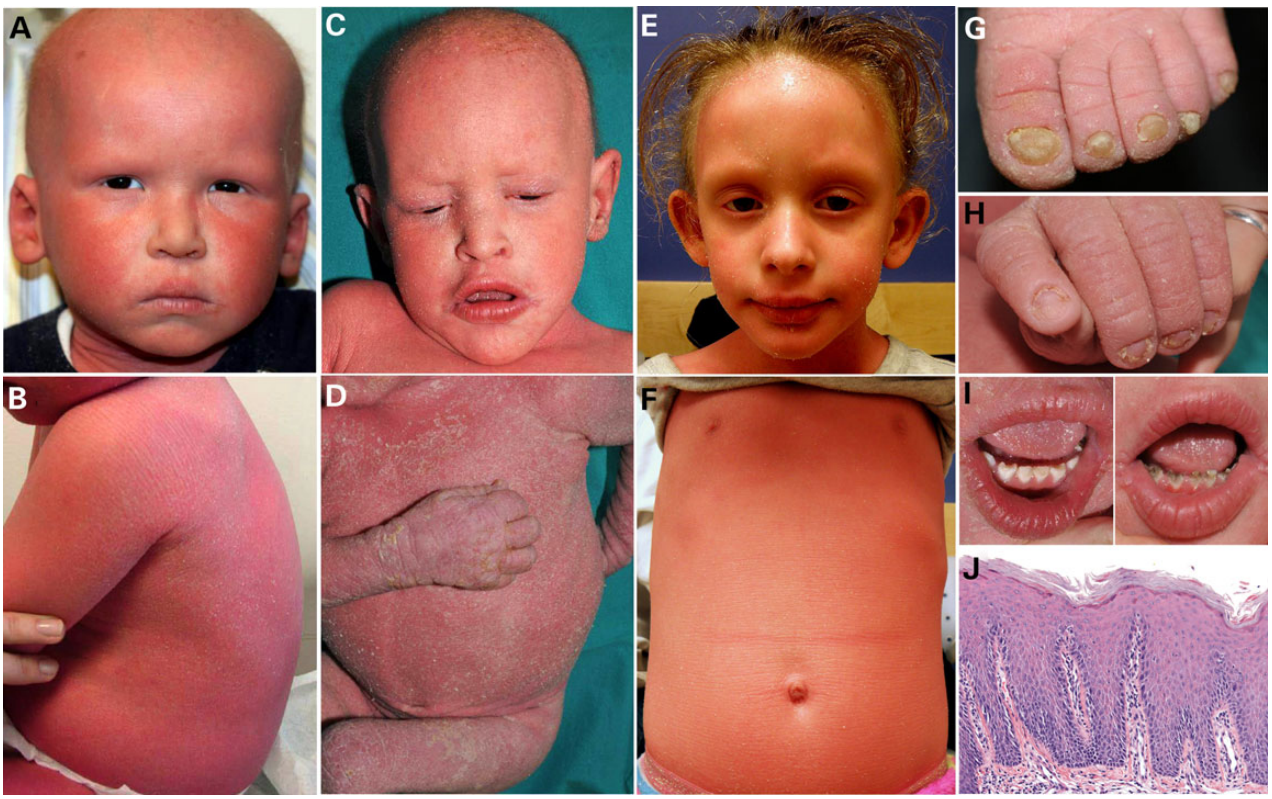

Figure 1. EKC syndrome features erythrokeratodermia, alopecia, and nail and dental abnormalities. (**A**, **C** and **E**) Faces of index cases 614, 244, and 380, respectively, show absence of eyebrow and eyelash hair, with minimal wispy scalp hair in cases 614 and 244 and sparse, curly hair in case 380. All show marked erythema and fine white scale. (**B**, **D** and **F**) Torso of each subject shows marked erythema and thickening of the skin with a corrugated appearance (erythokeratodermia), with fine, loosely adherent scale most prominent in case 244. (**G** and **H**) Onychodystrophy is present in each subject, with toenails of case 614 (G) and fingernails of case 244 (H) shown. (**I**) All subjects have chalky, soft enamel of primary teeth with progressive development of consumptive caries, evident in case 244 at 12 months (left) and 3 years (right). (**J**) Histopathology of affected skin shows acanthosis, hypogranulosis and compact hyperkeratosis with a psoriasiform appearance.

Index case 244 was noted to have severe congenital erythrokeratodermia, with scant eyebrow, eyelash and scalp hair (Fig. 1C and D). In infancy and early childhood he exhibited failure to thrive, dystrophy of all fingernails and toenails (Fig. 1H), fissuring and cracking of the palms and soles (Supplementary Material, Fig. S1B), and pruritus unresponsive to high doses of antihistamines. After age 1 he developed large hyperkeratotic plaques on the extensor surfaces of the extremities, and fissuring on ankles and wrists. Laboratory evaluations including complete blood count, biochemical and metabolic profiles, zinc, calcium, phosphorus, IgE, and vitamin D levels were within normal limits. Skin histopathology showed psoriasiform hyperplasia, parakeratosis, reduced granular layer, and intraepidermal neutrophils. At age 2 he developed progressive enamel defects, with lack of incisal edge, dentine exposure, and erythema of the gingival margin (Fig. 1I). X-rays revealed absence of many secondary teeth. Treatment with oral acitretin at doses ranging from 0.5 to 2 mg/kg throughout his life, a 2-month course of cyclosporine at 0.5 mg/kg, and multiple topical steroids failed to improve erythroderma or pruritus. Cardiac examination at 3.5 years revealed slight left ventricular dilation (Z +2.7) which progressed by age 7, with more pronounced left ventricular dilation (Z +4.9) and new right atrial dilation (Z +3.6), but preserved ventricular function. At birth he had four-limb spasticity that resolved over the first year of life, and photophobia that persisted, with development of large corneal opacities and severe visual impairment. There were no structural brain abnormalities noted on MRI, though developmental milestones are delayed, and at age 8 he is only able to pronounce simple sentences in a hoarse voice despite normal hearing.

Index case 380 was born with tight, red, cracked skin at birth and was noted to have sparse eyebrow, eyelash and scalp hair (Fig. 1E and F). She developed confluent erythrokeratodermia with peeling and fissuring of the palms and soles (Supplementary Material, Fig. S1C) and later grew sparse, coarse, wiry scalp hair without regrowth of eyebrows or eyelashes. She had dystrophy of all nails. Growth and development were normal, with height and weight consistently at the 75th percentile. Complete blood count was normal, without evidence of eosinophilia. Extensive RAST testing was negative except for cat allergy, and immunoglobulins including IgE were normal. Topical and systemic steroids worsened her erythroderma and pruritus. Oral acitretin improved scaling, though she remains erythrodermic. Dental examination revealed congenital absence of 11 secondary teeth, gingival recession and erythema, and poor mineralization of primary teeth, with widespread caries. Echocardiogram revealed a moderately dilated left ventricle (Z +4.4) with low normal systolic function. Histologic examination revealed psoriasiform hyperplasia and compact orthohyperkeratosis with a diminished granular layer.

DSP mutations

All three of these subjects were heterozygous for tightly clustered missense mutations in *DSP*: Q616P, H618P and L622P, respectively (Supplementary Material, Table S1). Sanger sequencing confirmed these mutations and showed that none were present in the unaffected parents of the subjects; thus, these mutations arose *de novo* (Supplementary Material, Fig. S2). None of these *DSP* mutations were found in ~2500 control exomes or in public databases of human variation, including the Broad Institute ExAC database which includes exome data from >60 000 unrelated individuals. All three mutations substitute proline for the native amino acid, and are clustered in exon 14 within a span encoding seven amino acids, at sites completely conserved in orthologs (Fig. 2A). The observation of three novel, clustered, *de novo* missense mutations in subjects with a consistent syndromic phenotype, which we term erythrokeratodermia-cardiomyopathy (EKC) syndrome, establishes the pathogenesis for this previously undescribed disorder is dominant mutation in *DSP*.

DSP is a 2871 amino acid plakin protein, consisting of six spectrin repeats (SRs) at its N-terminus, a rod domain which is largely absent from the isoform predominantly expressed in stratified epithelia (DSPII), and three tandem plakin repeat regions at the C-terminus (8,9). The N-terminal SRs, each of which consists of three α-helices forming an antiparallel triple-helical bundle and connects to a successive SR with an α-helical linker, are traditionally numbered by their homology to the SRs within plectin, another plakin protein; consequently the six SRs in DSP are labeled 3-6 and 8-9 (8). The C-terminal plakin repeats are labeled A-C. The N-terminus of DSP interacts with the PKPs and JUP, and the C-terminus mediates binding to intermediate filaments (9). Several other cardiac and/or cutaneous disorders, with both recessive and dominant inheritance, are known to be caused by mutations in *DSP* (Fig. 2B and Supplementary Material, Table S2). Both the type and the location of mutations determine the resulting phenotype.

The *DSP* mutations in our EKC syndrome subjects are tightly clustered within SR6, and the crystal structure for the N-terminal portion of DSP confirms close proximity within its third α-helix, close to the termination of the helix (Supplementary Material, Fig. S3) (8). All three mutations substitute the native residue with proline, which is a strong α-helix breaker and thereby likely disrupts the conserved helical structure (10). Unlike most SRs, which transition from one to the next within an α-helix, DSP SR6 and SR8 are connected by a non-helical linker. The EKC syndrome mutations occur within 5–11 amino acids of the native proline which terminates SR6. This clustering, and the consistent substitution of proline at mutation sites, suggest a common pathological mechanism unique to a small region of the large DSP protein.

Immunolocalization studies

To examine the consequence of these mutations, we stained normal skin and skin from an EKC syndrome subject (case 614, with *DSP* mutation Q616P) for desmosomal proteins DSP, DSG1, and JUP, and intermediate filament keratin KRT10. Staining revealed that while all are present in affected tissue and localize to intercellular junctions, overall signal intensity is reduced, with more diffuse localization. In particular, staining for DSP demonstrated that while normal skin shows strong suprabasal intercellular localization (Fig. 3A), suprabasal affected skin shows less intense intercellular staining with accumulation of membrane-associated and intracellular focal aggregates (Fig. 3B). DSG1 staining is strongly suprabasal at intercellular junctions in normal skin (Fig. 3C) and less tightly localized to intercellular junctions in affected tissue (Fig. 3D). Finally, JUP staining is tightly localized to intercellular junctions of suprabasal cells in normal skin (Fig. 3E) but in affected skin remains cytoplasmic and diffuse in basal cells, with weaker, more diffuse intercellular localization in suprabasal cells (Fig. 3F). Notably, staining for KRT10, a marker of differentiated keratinocytes, is retained in affected tissue and found to be strongly suprabasal and cytoplasmic, as in normal tissue (Fig. 3G and H).

To further explore the molecular phenotype of EKC syndrome mutations, the expression of gap junction protein Cx43 was examined. Staining of normal skin shows suprabasal punctate

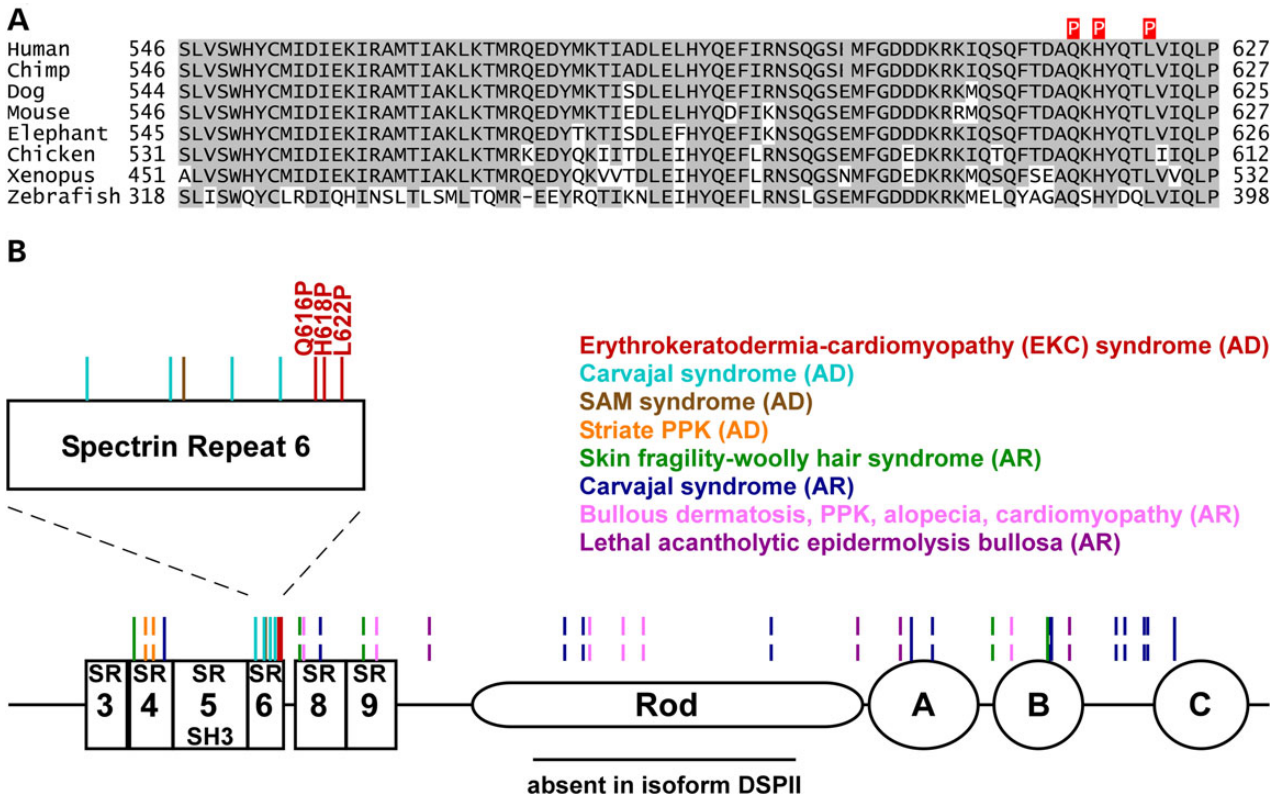

Figure 2. DSP conservation, domain structure and disease-causing mutations. (**A**) Human and orthologous protein sequences of the fourth spectrin domain of DSP, SR6. Conserved residues are shaded gray. Mutations causing EKC syndrome are above the alignment and shaded red. (**B**) DSP domains, including N-terminal spectrin repeats (SRs), the central rod domain (Rod), and C-terminal plakin repeats (A, B, C). SR5 contains an SH3 domain, and SRs 6 and 8 are bridged by a non-helical connector. Locations of mutations causing autosomal dominant (AD) and recessive (AR) human disease are shown with colored bars. A break in the bar indicates a truncating mutation. SR6 is enlarged, with mutations causing EKC syndrome indicated.

and linear intercellular membrane localization of Cx43 (Fig. 4A), whereas in affected skin, membrane staining intensity is diminished, and intercellular localization appears more diffuse (Fig. 4B). Additionally, wild-type and mutant GFP-labeled DSP constructs were expressed in primary human keratinocytes, and Cx43 membrane intensity was quantified. Both constructs expressing a *DSP* mutation (H618P, L622P) demonstrate Cx43 membrane intensity reduced to <80% of that observed in cells expressing wild-type DSP ($P < 0.01$) (Fig. 4C).

Electron microscopy studies

Transmission electron microscopy was performed to evaluate effects of *DSP* mutation on desmosome structure and lipid processing within the epidermis. Post-fixed tissue sections from index case 614 were treated with osmimum tetroxide to examine desmosomal structure, revealing that while desmosomes are present and have normal ultrastructural appearance in both basal and suprabasal epidermis, with electron dense plaques bordering a lucent central band, their number is reduced in suprabasal layers. This is likely due to marked aggregation of desmosomes either via shedding or internalization seen in spinous layer keratinocytes (Fig. 5A). Loss of desmosomes leads to widening of intercellular spaces in suprabasal cells (Fig. 5B). Despite desmosomal abnormalities, corneodesmosomes are intact and are normal both in structure and number (Fig. 5C). Marked deficits in lipid processing and secretion are also observed on ruthenium tetroxide staining, with premature secretion of lamellar bodies which have defective structure and supramolecular organization (Fig. 5D).

Discussion

We have shown that previously unreported, dominant, *de novo* missense mutations in *DSP* cause EKC syndrome, a previously undescribed syndromic form of erythrokeratodermia and cardiomyopathy, with additional consistent phenotypic features including dental enamel defects, absence of secondary teeth, and nail dystrophy. The genotypes, phenotypes, and changes in the expression and localization of desmosomal components in EKC syndrome are distinctly different from those of other disorders caused by mutation in either *DSP* or other genes encoding desmosomal proteins. The tight clustering of mutations within a short segment of SR6 and the consistent substitution of proline for the native residue suggest a unique and specific pathobiology.

Several distinct cardiac and/or limited-cutaneous phenotypes have been reported in subjects with recessive disease due to homozygosity or compound heterozygosity for *DSP* mutations. Premature nonsense and frameshift mutations (truncation mutations) cause recessive lethal acantholytic epidermolysis bullosa (OMIM #609638), characterized by severe skin fragility, universal alopecia, and profound fluid loss from skin erosions (11–13). However, in subjects compound heterozygous for truncation mutations in which one mutation lies within the portion of the rod domain absent from isoform DSPII, a syndrome of bullous dermatosis, palmoplantar keratoderma (PPK), alopecia

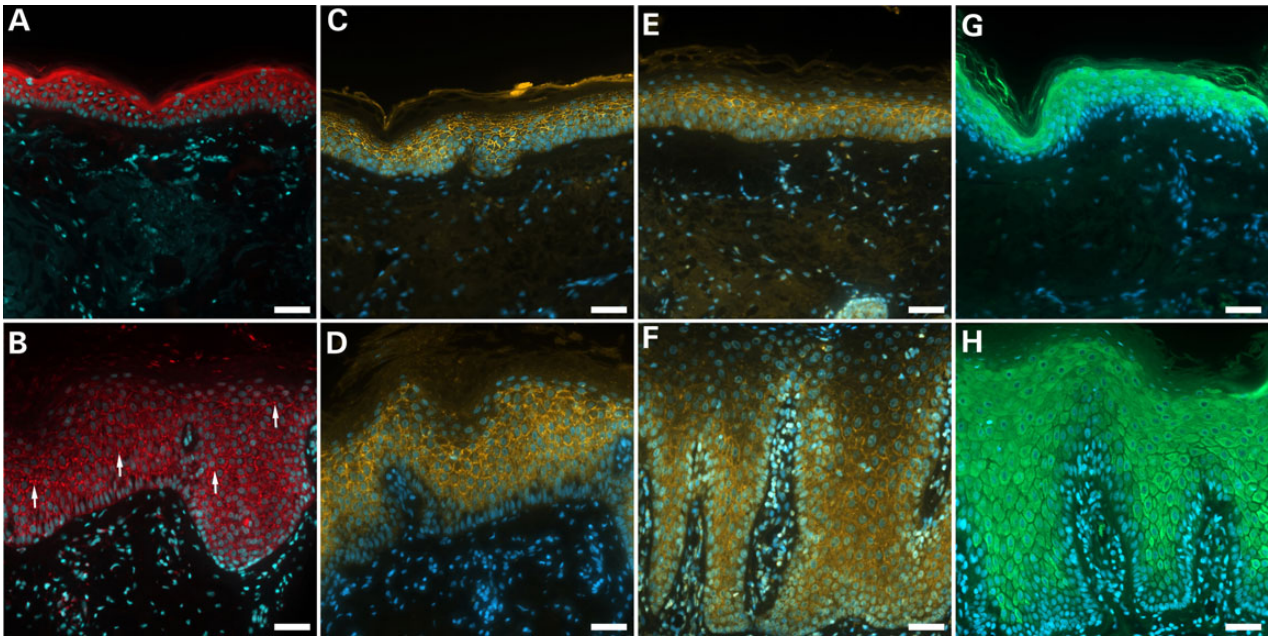

Figure 3. EKC syndrome mutations affect localization of desmosomal proteins but have no effect on keratin 10 expression. Skin tissue from normal abdomen (top panels) or from the back of index case 614 with *DSP* mutation Q616P (bottom panels) was employed for immunolocalization studies. DAPI nuclear counterstain is in blue in each panel. (**A** and **B**) Normal skin (A) shows prominent intercellular localization of desmoplakin (DSP, red) in suprabasal epidermis, while in affected tissue (B) intercellular localization is retained in suprabasal cells but is more diffuse, with intracellular and membrane-associated focal aggregates (white arrows). (**C** and **D**) Desmoglein 1 (DSG1, yellow) localizes tightly to intercellular junctions of suprabasal keratinocytes of normal tissue (C), but in affected skin (D) intercellular staining of suprabasal cells appears less tightly focused. (**E** and **F**) Junctional plakoglobin (JUP, yellow) localizes to suprabasal keratinocyte cell membranes in normal skin (E), but in affected tissue (F) suprabasal intercellular staining intensity is diminished and is more diffuse. (**G** and **H**) Keratin 10 (KRT10, green) is strongly expressed and cytoplasmic in suprabasal cells of normal tissue (G) and affected skin (H). Scale bars = 50 μm.

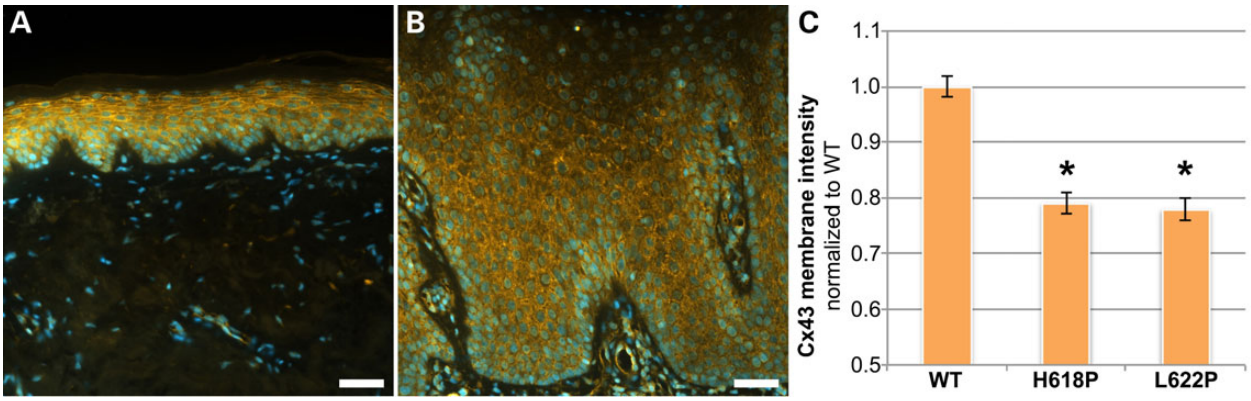

Figure 4. Connexin 43 localization is diminished in tissue and cells expressing EKC syndrome mutations. (**A** and **B**) Immunolocalization of connexin 43 (Cx43, yellow) in skin tissue is shown. DAPI nuclear counterstain is in blue. Normal skin (A) shows suprabasal punctate and linear intercellular membrane localization of Cx43, while in affected tissue from index case 614 with *DSP* mutation Q616P (B) staining intensity is diminished and intercellular localization appears more diffuse. Scale bars = 50 μm. (**C**) Wild-type (WT) and mutant (H618P, H622P) GFP-labeled DSP constructs were retrovirally expressed in normal human epidermal keratinocytes (NHEKs), and junctional Cx43 fluorescence intensity was quantified. A substantial decline (* = $P < 0.01$) is observed with EKC syndrome mutations. Data are from three independent experiments with $n > 70$ borders, normalized to wild-type. *P*-values were calculated using two-tailed, two-sample unequal variance Student's *t*-tests. Error bars represent SEM. Corresponding images are shown in Supplementary Material, Figure S4.

universalis, and severe cardiomyopathy is exhibited (14–16), and in subjects with truncation mutations exclusively within the variable portion of the rod domain or close to the C-terminus, recessive Carvajal syndrome (PPK with woolly hair and cardiomyopathy, OMIM #605676) is observed (17–22). Subjects compound heterozygous for a truncation mutation and a missense mutation, or homozygous for a missense mutation, have been described with variations of recessive Carvajal syndrome either more severe (consistent early cardiac lethality, with blistering) (21,23,24) or more mild (palmar-only or minor PPK, curly to woolly hair) (22,25), and with recessive skin fragility-woolly hair syndrome (OMIM #607655), distinguished from Carvajal by blistering and lack of cardiac involvement (26–28).

Dominant phenotypes characterized by either cardiac or cutaneous disease have been reported to result from heterozygosity for a *DSP* mutation. Heterozygosity for missense or truncation mutations scattered throughout the protein are associated with arrhythmogenic cardiomyopathy without skin findings (OMIM

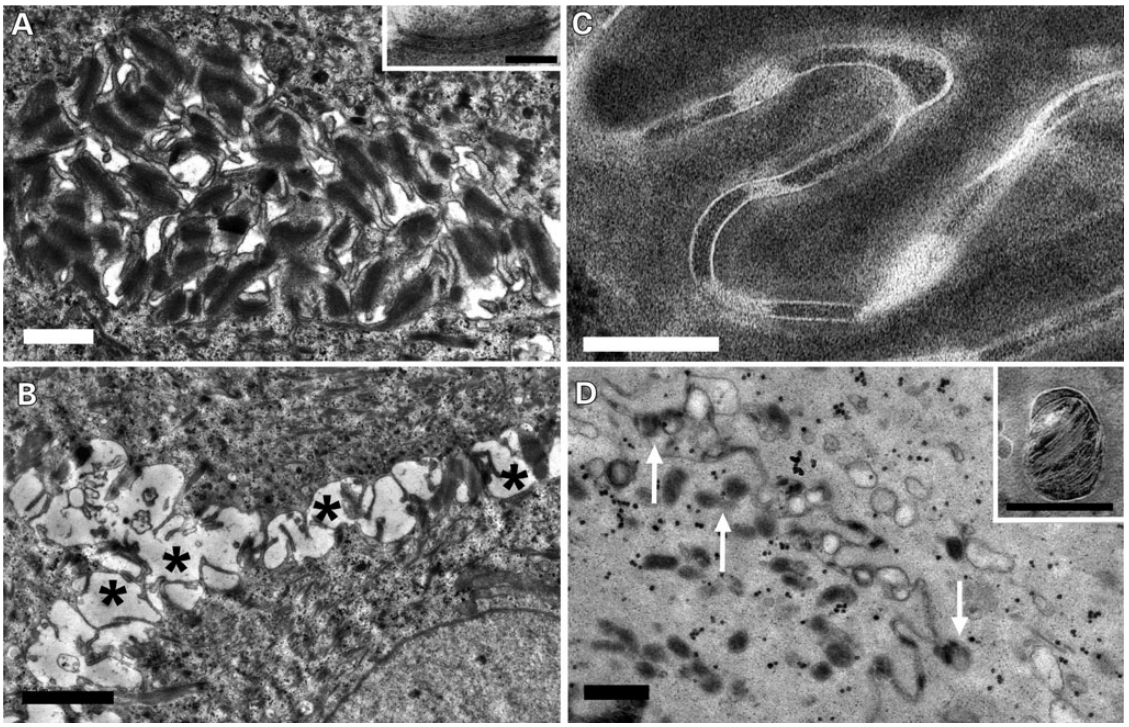

Figure 5. Desmosome aggregation, widening of intercellular spaces, and lipid secretory defects in EKC syndrome. Electron microscopy images of post-fixed tissue from index case 614 (*DSP* mutation Q616P), treated with osmium tetroxide (**A** and **B**) or ruthenium tetroxide (**C** and **D**), are shown. (A) At the level of the stratum spinosum, desmosomes are internalized or shed to form large aggregates, though they retain normal structure with a central band when membrane-localized (inset). (B) Desmosome internalization leads to widening of intracellular spaces (asterisks). (C) Despite abnormal desmosome processing, corneodesmosomes appear normal in both number and internal structure. (D) Loss of desmosomes leads to abnormalities in lamellar body secretion, with premature secretion of lamellar bodies (arrows) which have defective structure and supramolecular organization (inset). Scale bars: A = 1 μm (inset 0.2 μm), B = 2 μm, C = 200 nm, D = 0.5 nm (inset = 0.2 nm).

#607450) (29,30), which can also be caused by mutations in other desmosomal components (DSG2, DSC2, PKP2, JUP) (2). Heterozygous truncation mutations within SR4, including Q331X and a splice site mutation that results in retention of intron 7 and termination 25 amino acids after the exon 7 donor splice site, cause dominant striate PPK (OMIM #612908) (31,32). Additionally, a heterozygous mutation in SR6 in a single individual was reported to cause dominant severe dermatitis, multiple allergies, and metabolic wasting (SAM) syndrome, without evidence of cardiac disease (33). In three other families described to date, SAM syndrome is recessive and caused by homozygosity for a truncating mutation in *DSG1* (34,35).

While other dominant *DSP* mutations cause disease with both cardiac and cutaneous components, the phenotype is significantly different from that of EKC syndrome. Heterozygosity for an in-frame insertion or a missense mutation within SR6 has been shown to cause dominant Carvajal syndrome, which features limited skin involvement (isolated PPK) with woolly hair and cardiomyopathy (OMIM #615821) (36–39).

We show that dominant mutations in *DSP* cause EKC syndrome, characterized by erythrokeratodermia and progressive cardiomyopathy. In addition to the distinct clinical phenotype in EKC, unique pathobiology was also observed when compared to the effects of other mutations within the spectrin repeats of *DSP*.

Consistent with our findings, other *DSP* mutations also lead to reduced Cx43 membrane localization in epithelial cells. These include truncating mutations causing bullous dermatosis, PPK, alopecia, and cardiomyopathy (Q673X in SR8, and Q1446X in the DSPI-specific portion of the Rod domain) (14) in which reduced expression of both JUP and Cx43 at epidermal junctional sites was observed in the skin of one subject. Similarly, a missense mutation from a subject with recessive skin fragility-woolly hair syndrome (N287K, within SR4) severely disrupts normal membrane localization of DSP, impairs PKP1 and JUP binding and cell-cell adhesive strength, and reduces Cx43 membrane localization when expressed in culture. The same study shows that Cx43 localization is also disrupted by mutations from subjects with dominant arrhythmogenic cardiomyopathy (N458Y and I533T, both within the SH3 domain of SR5), but unlike N287K, neither affected normal membrane localization of DSP itself, nor cell-cell adhesive strength (3).

There is a single report of dermatitis, elevated IgE, eosinophilia, and severe allergies without cardiomyopathy in a subject with SAM syndrome due to an H586P *DSP* mutation, which like our mutations is dominant and lies within SR6, but elevated IgE, eosinophilia, and allergy are not found in any EKC syndrome subject. Immunolocalization studies further differentiate these syndromes. In the SAM syndrome case there is loss of DSP membrane localization with cytoplasmic aggregation, and near complete ablation of DSG1 and KRT10 expression (33). By contrast, in EKC syndrome we find intercellular localization of DSP with focal membrane-associated aggregates, slightly reduced intercellular DSG1 localization, and normal KRT10 expression. The retained DSG1 expression in EKC syndrome skin, versus its ablation in SAM syndrome skin, is consistent with the other known cause of SAM syndrome: recessive loss of function mutations in *DSG1* (34,35). Furthermore, DSG1 promotes epidermal differentiation by suppressing EGFR signaling (40) and ERK activation (41); its loss is therefore consistent with the concomitant

loss of KRT10, a marker of epidermal differentiation, observed in SAM syndrome skin (33). By contrast, EKC syndrome skin retains normal KRT10 expression. The extent to which a *DSP* mutation perturbs DSG1 function and epidermal differentiation is likely a critical molecular mechanism behind the presence of immunologic findings in SAM syndrome, and the absence of these phenotypic features in EKC syndrome.

DSP SR6 is a hotspot for dominant mutations that cause cutaneous disease. In fact, with the exception of the truncation mutations in SR4 that cause striate PPK, all dominant, cutaneous disease-causing mutations in *DSP* are missense substitutions or in-frame insertions within SR6. Notably, none of the disorders previously known to be caused by *DSP* mutations feature the profound erythrokeratodermia and ichthyosis observed in our cohort. Additional differences compared to Carvajal syndrome, the dominant form of which is also caused by substitution mutations in *DSP* SR6, include a more mild PPK, more profound and consistent alopecia, itch, and variable features of failure to thrive, developmental delay, visual impairment, and hoarse voice observed in our EKC syndrome subjects.

While the phenotypic differences between Carvajal, SAM, and EKC syndromes are apparent, explanations for genotype-phenotype correlations are more difficult. Both the dominant Carvajal mutations and the SAM mutation occur earlier within SR6 than the EKC mutations, and are distributed across a larger region, between the first and second α-helix to the N-terminal end of the third α-helix (Supplementary Material, Fig. S3). The SAM mutation and one of four Carvajal mutations introduce a proline substitution and likely helix-breaker into the second α-helix, and another Carvajal mutation inserts ten residues into sequence encoding the start of the third α-helix. While it might have been tempting to hypothesize simply that earlier disruptions in SR6 lead to Carvajal syndrome whereas later disruptions cause EKC syndrome, the proximity and similarity of the recently reported SAM mutation (H586P) to one of the Carvajal mutations (L583P) reveals that even subtle genotypic differences in SR6 can result in substantial phenotypic differences.

By contrast, dominant mutations (both truncating and missense) scattered throughout the protein cause arrhythmogenic cardiomyopathy, without a cutaneous component. At least some of these appear incompletely penetrant, as reports of skin fragility-woolly hair syndrome subjects with one truncating mutation describe absence of apparent cardiac disease (26,28) and some adult carriers for truncating *DSP* mutations in families with recessive disease have received extensive cardiac workups and are apparently without a cardiac phenotype (11). The original reports of striate PPK due to truncating mutations in SR4 did not describe a cardiac phenotype, although one of the two mutations has subsequently been reported to cause heart disease (25). In this context, one could hypothesize that haploinsufficiency for full-length DSP predisposes to cardiomyopathy, but is not overtly pathogenic in the skin and other organ systems, with the exception of truncations occurring specifically within SR4 which cause cutaneous disease isolated to the palms and soles. Since mutations that cause arrhythmogenic cardiomyopathy alone occur throughout DSP, both 5′ and 3′ to those causing striate PPK, the phenotypic differences cannot be explained by merely how N-terminal the mutation is, and are likely also related to the exact nature of mutant transcripts and the extent of their expression; nonsense-mediated decay is incomplete for some *DSP* mutations, with demonstrated expression of truncated polypeptides (11).

While much is known about cardiac and/or cutaneous disease resulting from mutation in desmosomal components, cardiac defects have not been previously associated with generalized erythrokeratodermia, nor with severe ichthyosis. Notably, EKC syndrome is due to tightly clustered mutations in a short span of the SR6 domain of DSP with consistent substitution of proline for the native residue, suggesting a unique and specific pathobiology leading to widespread erythrokeratodermia. Prior to our discovery of pathogenic *DSP* mutations, neither case 244 nor case 380 had been diagnosed with cardiomyopathy; case 380 had never previously received a cardiac workup. The subsequent diagnosis of cardiac defects in both of these subjects highlights the critical, potentially life-saving importance of this genetic discovery, which necessitates consideration of cardiac disease and genetic diagnosis in all patients presenting with erythrokeratodermia in clinical practice.

Materials and Methods

DOK cohort

The Yale Human Investigation Committee approved the study protocol, consistent with the Declaration of Helsinki guidelines, and subjects provided verbal and written informed consent. There were 496 kindreds in the DOK cohort at the time of manuscript preparation. Genomic DNA was isolated from blood using a standard phenol-chloroform protocol.

Exome sequencing

Bar-coded DNA libraries were prepared and exome capture was performed (EZ Exome 2.0, Roche, Basel, Switzerland) by the Yale Center for Genome Analysis. Illumina HiSeq 2000 and 2500 instruments were used for sequencing samples pooled 6 per lane, with 75 bp paired-end reads. Resulting reads were aligned to the human reference genome (hg19) with ELAND software (Illumina, San Diego, CA), sequence was trimmed to targeted intervals, PCR duplicates were removed, and single nucleotide and indel variants were identified using SAMtools software. Variants were annotated for functional impact, and filtered to examine coding mutations with SAMtools quality scores ≥50 and to exclude frequent variants present in dbSNP, 1000 Genomes, the NHLBI exome database, and 2577 control exomes. The Broad Institute ExAC database was used to further assess mutations for novelty. Aligned reads were examined with the Broad Institute Integrative Genomics Viewer (IGV).

Sanger sequencing

Verification of *DSP* mutations and sequencing of parental DNA was performed via PCR using Kapa 2G Fast polymerase (Kapa Biosystems, Woburn, MA) and Sanger sequencing. Primers were designed with ExonPrimer and SNPmasker.

Antibodies

The following primary antibodies were used: for tissue immunofluorescence, guinea pig anti-DSP (1:50, DP-1, Progen), mouse anti-DSG1 (1:10, 61002, Progen), rabbit anti-JUP (1:100, ab15153, Abcam), mouse anti-KRT10 (1:200, sc-53252, Santa Cruz), and rabbit anti-Cx43 (1:100, ab11370, Abcam); for NHEK immunofluorescence, mouse anti-GFP (JL8, Living Colors) and rabbit anti-Cx43 (AB1728; EMD Millipore). The following secondary antibodies were used: for tissue immunofluorescence, cyanine-conjugated donkey anti-guinea pig (1:200 Cy5), anti-mouse (1:800, Cy3 for DSG1; 1:200, Cy2 for KRT10), and anti-rabbit (1:800 Cy3) (Jackson ImmunoResearch);

for NHEK immunofluorescence, Alexa Fluor-conjugated goat anti-mouse (488) and anti-rabbit (568) (Invitrogen).

Tissue immunofluorescence

5 μm FFPE tissue sections were deparaffinized with a xylene-ethanol gradient and rinsed in PBS. Antigen retrieval was performed by immersion in modified citrate buffer (10 mM sodium citrate, 0.05% Tween 20, pH 6.0) for 20 min in a steamer. Slides were cooled and rinsed in PBS. Tissue was permeabilized with 10% donkey serum/1% BSA/0.1% Triton X100 for 10 min, and blocked with 10% donkey serum/1% BSA for 1 h. Slides were incubated with primary and secondary antibodies and DAPI nuclear counterstain for 2 h, 1 h and 3 min respectively, with three PBS washes following incubations, and mounted with Mowiol/1% n-propyl gallate (Polysciences).

Generation of DSPII constructs

Nucleotides 3584-5380 of a GFP-tagged, full-length, wild-type human DSPI construct were spliced out to generate a GFP-tagged DSPII construct (42), which was cloned into the pENTR/D-TOPO Gateway vector (Invitrogen) and inserted into the LZRS retroviral vector to generate a retroviral DSPII-GFP construct. Site-specific mutant DSPII-GFP constructs were generated using the QuikChange II XL Site-Directed Mutagenesis kit (Agilent Technologies).

Cell culture

Normal human epidermal keratinocytes (NHEKs) were cultured in M154 medium (Invitrogen) at 0.07 mM Ca^{2+} and supplemented with human keratinocyte growth supplement and gentamycin/amphotericin B solution (Invitrogen). To induce differentiation, NHEKs were seeded onto glass coverslips, grown to confluence, and switched to high Ca^{2+} medium 154 (containing 1.2 mM $CaCl_2$) for 24 h. The Phoenix packaging cell line was maintained in DMEM (Mediatech) supplemented with 10% FBS (Atlanta Biologicals) and penicillin/streptomycin solution (Sigma-Aldrich). Phoenix cells were transfected with DSPII-GFP constructs and switched into 1 μg/ml puromycin selection media 48 h after transfection. Following drug selection, cells were incubated at 32°C for 16–24 h and viral supernatant was collected and concentrated using Amicon Ultra-15 Centrifugal Filter units (EMD Millipore). To infect NHEKs, viral supernatant with 4 μg/ml polybrene was added to undifferentiated cells for 90 min at 32°C, followed by two PBS washes and a return to 37°C with fresh media.

NHEK immunofluorescence

NHEKs plated onto glass coverslips were washed in PBS and fixed by submersion in anhydrous methanol for 2 min at –20°C. Cells were incubated with primary and secondary antibodies for 1 h and 30 min respectively, with three PBS washes following incubations. Coverslips were mounted onto slides using polyvinyl alcohol (Sigma-Aldrich). ImageJ software was used to quantify cell junction localization of DSPII-GFP and Cx43. Data was normalized to wild-type. P-values were calculated using two-tailed, two-sample unequal variance Student's *t*-tests. Error bars represent SEM.

Supplementary Material

Supplementary Material is available at *HMG* online.

Acknowledgements

We thank the subjects and their families, and Dane's Friends for FIRST, for their invaluable contribution to this work. We thank Nemanja Rodic for dermatopathology assistance, and Carol Nelson-Williams and Kaya Bilguvar for technical assistance.

Conflict of Interest statement. None declared.

Funding

This work was supported by a Doris Duke Charitable Foundation Clinical Scientist Development Award to K.A.C., a Research Grant from the Foundation for Ichthyosis & Related Skin Types Inc. (FIRST) funded by the Ambrose Monell and Lennox Foundations, an NIH grant to K.J.G. (NIH R37 AR043380), the Yale Center for Mendelian Genomics (NIH U54 HG006504), and the Yale Center for Clinical Investigation (NIH UL1 TR000142).

References

1. Samuelov, L. and Sprecher, E. (2015) Inherited desmosomal disorders. *Cell Tissue Res.*, **360**, 457–475.
2. Patel, D.M. and Green, K.J. (2014) Desmosomes in the heart: a review of clinical and mechanistic analyses. *Cell Commun. Adhes.*, **21**, 109–128.
3. Patel, D.M., Dubash, A.D., Kreitzer, G. and Green, K.J. (2014) Disease mutations in desmoplakin inhibit Cx43 membrane targeting mediated by desmoplakin-EB1 interactions. *J. Cell Biol.*, **206**, 779–797.
4. Shaw, R.M., Fay, A.J., Puthenveedu, M.A., von Zastrow, M., Jan, Y.N. and Jan, L.Y. (2007) Microtubule plus-end-tracking proteins target gap junctions directly from the cell interior to adherens junctions. *Cell*, **128**, 547–560.
5. Laird, D.W. (2014) Syndromic and non-syndromic disease-linked Cx43 mutations. *FEBS Lett.*, **588**, 1339–1348.
6. Laird, D.W. (2006) Life cycle of connexins in health and disease. *Biochem. J.*, **394**, 527–543.
7. Martin, P.E., Easton, J.A., Hodgins, M.B. and Wright, C.S. (2014) Connexins: sensors of epidermal integrity that are therapeutic targets. *FEBS Lett.*, **588**, 1304–1314.
8. Choi, H.J. and Weis, W.I. (2011) Crystal structure of a rigid four-spectrin-repeat fragment of the human desmoplakin plakin domain. *J. Mol. Biol.*, **409**, 800–812.
9. Nekrasova, O. and Green, K.J. (2013) Desmosome assembly and dynamics. *Trends Cell Biol.*, **23**, 537–546.
10. Altmann, K.H., Wójcik, J., Vásquez, M. and Scheraga, H.A. (1990) Helix-coil stability constants for the naturally occurring amino acids in water. XXIII. Proline parameters from random poly (hydroxybutylglutamine-co-L-proline). *Biopolymers*, **30**, 107–120.
11. Jonkman, M.F., Pasmooij, A.M., Pasmans, S.G., van den Berg, M.P., Ter Horst, H.J., Timmer, A. and Pas, H.H. (2005) Loss of desmoplakin tail causes lethal acantholytic epidermolysis bullosa. *Am. J. Hum. Genet.*, **77**, 653–660.
12. Bolling, M.C., Veenstra, M.J., Jonkman, M.F., Diercks, G.F., Curry, C.J., Fisher, J., Pas, H.H. and Bruckner, A.L. (2010) Lethal acantholytic epidermolysis bullosa due to a novel homozygous deletion in DSP: expanding the phenotype and implications for desmoplakin function in skin and heart. *Br. J. Dermatol.*, **162**, 1388–1394.
13. Hobbs, R.P., Han, S.Y., van der Zwaag, P.A., Bolling, M.C., Jongbloed, J.D., Jonkman, M.F., Getsios, S., Paller, A.S. and Green, K.J. (2010) Insights from a desmoplakin mutation identified

in lethal acantholytic epidermolysis bullosa. *J. Invest. Dermatol.*, **130**, 2680–2683.
14. Asimaki, A., Syrris, P., Ward, D., Guereta, L.G., Saffitz, J.E. and McKenna, W.J. (2009) Unique epidermolytic bullous dermatosis with associated lethal cardiomyopathy related to novel desmoplakin mutations. *J. Cutan. Pathol.*, **36**, 553–559.
15. Tanaka, A., Lai-Cheong, J.E., Café, M.E., Gontijo, B., Salomão, P.R., Pereira, L. and McGrath, J.A. (2009) Novel truncating mutations in PKP1 and DSP cause similar skin phenotypes in two Brazilian families. *Br. J. Dermatol.*, **160**, 692–697.
16. Antonov, N.K., Kingsbery, M.Y., Rohena, L.O., Lee, T.M., Christiano, A., Garzon, M.C. and Lauren, C.T. (2015) Early-onset heart failure, alopecia, and cutaneous abnormalities associated with a novel compound heterozygous mutation in desmoplakin. *Pediatr. Dermatol.*, **32**, 102–108.
17. Norgett, E.E., Hatsell, S.J., Carvajal-Huerta, L., Cabezas, J.C., Common, J., Purkis, P.E., Whittock, N., Leigh, I.M., Stevens, H.P. and Kelsell, D.P. (2000) Recessive mutation in desmoplakin disrupts desmoplakin-intermediate filament interactions and causes dilated cardiomyopathy, woolly hair and keratoderma. *Hum. Mol. Genet.*, **9**, 2761–2766.
18. Uzumcu, A., Norgett, E.E., Dindar, A., Uyguner, O., Nisli, K., Kayserili, H., Sahin, S.E., Dupont, E., Severs, N.J., Leigh, I.M. *et al.* (2006) Loss of desmoplakin isoform I causes early onset cardiomyopathy and heart failure in a Naxos-like syndrome. *J. Med. Genet.*, **43**, e5.
19. Williams, T., Machann, W., Kühler, L., Hamm, H., Müller-Höcker, J., Zimmer, M., Ertl, G., Ritter, O., Beer, M. and Schönberger, J. (2011) Novel desmoplakin mutation: juvenile biventricular cardiomyopathy with left ventricular noncompaction and acantholytic palmoplantar keratoderma. *Clin. Res. Cardiol.*, **100**, 1087–1093.
20. Rasmussen, T.B., Hansen, J., Nissen, P.H., Palmfeldt, J., Dalager, S., Jensen, U.B., Kim, W.Y., Heickendorff, L., Mølgaard, H., Jensen, H.K. *et al.* (2013) Protein expression studies of desmoplakin mutations in cardiomyopathy patients reveal different molecular disease mechanisms. *Clin. Genet.*, **84**, 20–30.
21. Molho-Pessach, V., Sheffer, S., Siam, R., Tams, S., Siam, I., Awwad, R., Babay, S., Golender, J., Simanovsky, N., Ramot, Y. *et al.* (2015) Two novel homozygous desmoplakin mutations in Carvajal syndrome. *Pediatr. Dermatol.*, **32**, 641–646.
22. Pigors, M., Schwieger-Briel, A., Cosgarea, R., Diaconeasa, A., Bruckner-Tuderman, L., Fleck, T. and Has, C. (2015) Desmoplakin mutations with palmoplantar keratoderma, woolly hair and cardiomyopathy. *Acta Derm. Venereol.*, **95**, 337–340.
23. Alcalai, R., Metzger, S., Rosenheck, S., Meiner, V. and Chajek-Shaul, T. (2003) A recessive mutation in desmoplakin causes arrhythmogenic right ventricular dysplasia, skin disorder, and woolly hair. *J. Am. Coll. Cardiol.*, **42**, 319–327.
24. Mahoney, M.G., Sadowski, S., Brennan, D., Pikander, P., Saukko, P., Wahl, J., Aho, H., Heikinheimo, K., Bruckner-Tuderman, L., Fertala, A. *et al.* (2010) Compound heterozygous desmoplakin mutations result in a phenotype with a combination of myocardial, skin, hair, and enamel abnormalities. *J. Invest. Dermatol.*, **130**, 968–978.
25. Christensen, A.H., Benn, M., Bundgaard, H., Tybjaerg-Hansen, A., Haunso, S. and Svendsen, J.H. (2010) Wide spectrum of desmosomal mutations in Danish patients with arrhythmogenic right ventricular cardiomyopathy. *J. Med. Genet.*, **47**, 736–744.
26. Whittock, N.V., Wan, H., Morley, S.M., Garzon, M.C., Kristal, L., Hyde, P., McLean, W.H., Pulkkinen, L., Uitto, J., Christiano, A.M. *et al.* (2002) Compound heterozygosity for non-sense and mis-sense mutations in desmoplakin underlies skin fragility/woolly hair syndrome. *J. Invest. Dermatol.*, **118**, 232–238.
27. Al-Owain, M., Wakil, S., Shareef, F., Al-Fatani, A., Hamadah, E., Haider, M., Al-Hindi, H., Awaji, A., Khalifa, O., Baz, B. *et al.* (2011) Novel homozygous mutation in DSP causing skin fragility-woolly hair syndrome: report of a large family and review of the desmoplakin-related phenotypes. *Clin. Genet.*, **80**, 50–58.
28. Smith, F.J., Wilson, N.J., Moss, C., Dopping-Hepenstal, P. and McGrath, J. (2012) Compound heterozygous mutations in desmoplakin cause skin fragility and woolly hair. *Br. J. Dermatol.*, **166**, 894–896.
29. Rampazzo, A., Nava, A., Malacrida, S., Beffagna, G., Bauce, B., Rossi, V., Zimbello, R., Simionati, B., Basso, C., Thiene, G. *et al.* (2002) Mutation in human desmoplakin domain binding to plakoglobin causes a dominant form of arrhythmogenic right ventricular cardiomyopathy. *Am. J. Hum. Genet.*, **71**, 1200–1206.
30. van der Zwaag, P.A., Jongbloed, J.D., van den Berg, M.P., van der Smagt, J.J., Jongbloed, R., Bikker, H., Hofstra, R.M. and van Tintelen, J.P. (2009) A genetic variants database for arrhythmogenic right ventricular dysplasia/cardiomyopathy. *Hum. Mutat.*, **30**, 1278–1283.
31. Armstrong, D.K., McKenna, K.E., Purkis, P.E., Green, K.J., Eady, R.A., Leigh, I.M. and Hughes, A.E. (1999) Haploinsufficiency of desmoplakin causes a striate subtype of palmoplantar keratoderma. *Hum. Mol. Genet.*, **8**, 143–148.
32. Whittock, N.V., Ashton, G.H., Dopping-Hepenstal, P.J., Gratian, M.J., Keane, F.M., Eady, R.A. and McGrath, J.A. (1999) Striate palmoplantar keratoderma resulting from desmoplakin haploinsufficiency. *J. Invest. Dermatol.*, **113**, 940–946.
33. McAleer, M.A., Pohler, E., Smith, F.J., Wilson, N.J., Cole, C., MacGowan, S., Koetsier, J.L., Godsel, L.M., Harmon, R.M., Gruber, R. *et al.* (2015) Severe dermatitis, multiple allergies, and metabolic wasting syndrome caused by a novel mutation in the N-terminal plakin domain of desmoplakin. *J. Allergy Clin. Immunol.*, **136**, 1268–1276.
34. Samuelov, L., Sarig, O., Harmon, R.M., Rapaport, D., Ishida-Yamamoto, A., Isakov, O., Koetsier, J.L., Gat, A., Goldberg, I., Bergman, R. *et al.* (2013) Desmoglein 1 deficiency results in severe dermatitis, multiple allergies and metabolic wasting. *Nat. Genet.*, **45**, 1244–1248.
35. Has, C., Jakob, T., He, Y., Kiritsi, D., Hausser, I. and Bruckner-Tuderman, L. (2015) Loss of desmoglein 1 associated with palmoplantar keratoderma, dermatitis and multiple allergies. *Br. J. Dermatol.*, **172**, 257–261.
36. Norgett, E.E., Lucke, T.W., Bowers, B., Munro, C.S., Leigh, I.M. and Kelsell, D.P. (2006) Early death from cardiomyopathy in a family with autosomal dominant striate palmoplantar keratoderma and woolly hair associated with a novel insertion mutation in desmoplakin. *J. Invest. Dermatol.*, **126**, 1651–1654.
37. Chalabreysse, L., Senni, F., Bruyère, P., Aime, B., Ollagnier, C., Bozio, A. and Bouvagnet, P. (2011) A new hypo/oligodontia syndrome: Carvajal/Naxos syndrome secondary to desmoplakin-dominant mutations. *J. Dent. Res.*, **90**, 58–64.
38. Keller, D.I., Stepowski, D., Balmer, C., Simon, F., Guenthard, J., Bauer, F., Itin, P., David, N., Drouin-Garraud, V. and Fressart, V. (2012) De novo heterozygous desmoplakin mutations leading to Naxos-Carvajal disease. *Swiss Med. Wkly.*, **142**, w13670.
39. Boulé, S., Fressart, V., Laux, D., Mallet, A., Simon, F., de Groote, P., Bonnet, D., Klug, D. and Charron, P. (2012) Expanding the phenotype associated with a desmoplakin dominant mutation: Carvajal/Naxos syndrome associated with leukonychia and oligodontia. *Int. J. Cardiol.*, **161**, 50–52.

40. Getsios, S., Simpson, C.L., Kojima, S., Harmon, R., Sheu, L.J., Dusek, R.L., Cornwell, M. and Green, K.J. (2009) Desmoglein 1-dependent suppression of EGFR signaling promotes epidermal differentiation and morphogenesis. *J. Cell Biol.*, **185**, 1243–1258.
41. Harmon, R.M., Simpson, C.L., Johnson, J.L., Koetsier, J.L., Dubash, A.D., Najor, N.A., Sarig, O., Sprecher, E. and Green, K.J. (2013) Desmoglein-1/Erbin interaction suppresses ERK activation to support epidermal differentiation. *J. Clin. Invest.*, **123**, 1556–1570.
42. Godsel, L.M., Hsieh, S.N., Amargo, E.V., Bass, A.E., Pascoe-McGillicuddy, L.T., Huen, A.C., Thorne, M.E., Gaudry, C.A., Park, J.K., Myung, K. *et al.* (2005) Desmoplakin assembly dynamics in four dimensions: multiple phases differentially regulated by intermediate filaments and actin. *J. Cell Biol.*, **171**, 1045–1059.